Journal of Applied Analysis and Computation
Volume 16, Number 1, February 2026, 136–154
Website:http://www.jaac-online.com
DOI:10.11948/20240542

# ANALYSIS OF THE KINETIC PROPERTIES OF THE DISCRETE FOREST DISEASE AND INSECT PEST MODELS*

**Jiarui Zhang[1], Wei Li[1] and Mi Wang[1,†]**

**Abstract** In this paper, we study the dynamic behavior of discrete forest disease and pest model-spruce aphid model, analyze the properties of the dynamics by using the difference equation theory, including the existence of equilibrium points in the system model, and further analyze the stability and instability conditions of these equilibrium points. In addition, the step h is selected as the bifurcation parameter using the central manifold theorem to analyze the Flip bifurcation and Hopf bifurcation at the equilibrium point, and prove the chaos of the system through the maximum Lyapunov diagram. In order to verify the theoretical proof, the system model is simulated numerically to draw relevant conclusions.

**Keywords** Discrete forest disease and insect pest models, Flip bifurcation, Hopf bifurcation, chaos analysis.

**MSC(2010)** 34C23, 37N25.

## 1. Introduction

With the rapid development of industry and agriculture and the acceleration of the process of economic globalization, the problem of forest diseases and pests has gradually emerged and brought adverse effects on the forest environment. The problem of forest diseases and pests is a hot issue in international and domestic research on forest environment, and scientists from all over the world have done a lot of research on forest diseases and pests [1,11,16,19,25,28–30,34], especially spruce aphids [2, 5–7, 12, 13, 17, 21–24, 26]. As a major pest in coniferous forests, the spruce aphid's explosive reproduction can lead to large-scale defoliation of spruce, seriously weakening the carbon sink capacity and ecological function of forests. Climate change has further exacerbated the suddenness and unpredictability of the pests and diseases, and the traditional means of chemical control is facing serious challenges due to environmental pollution and bioresistance, and other problems.

Ludwig et al. [18], proposed a model to separate the time scales of slow spruce regeneration from the rapid population dynamics of budworm larvae and their predators, and they used a so-called logistic model to study the finite food dynamics of budworms in the absence of predators, S. J. Crute [3], established a computer simulation model of the population dynamics of Elatobium abietinum, which provides a good research tool for further study of the population dynamics of Elatobium abietinum. And Li Aihua et al. [14], used differential equations and control theory to study the effect of the use of pesticides on the dynamic characteristics of the interaction model

†The corresponding author.
[1]Department of Mathematics, Northeast Forestry University, Harbin 150040, China
*The authors were supported by Fundamental Research Funds for the Central Universities: 60201523050.
Email: 401095643@qq.com(J. Zhang), lwmath@nefu.edu.cn(W. Li),
nefulxywangmi@163.com(M. Wang)

between a class of spruce aphids and their natural enemies, including the number of positive equilibrium points in the control model of spruce aphids-natural enemies-insecticides, and the relationship between the stability of the positive equilibrium points and the amount of pesticides used.

In the ecological community, the survival and development of many biological populations and the change of their numbers do not occur continuously, but many biological system models are continuous system models. In order to study the nature of the population and analyze it accordingly, the continuous system model is usually discretized [10, 15, 27, 31–33], and the discretized system model is more helpful to analyze the properties of the biological population, and at the same time, it can also ensure that the properties of the biological population will not change in the research process, and even destroy the original good biological population properties. In view of the relative lack of research on discrete models of forest diseases and pests, it is of great importance to study these discrete models directly.

$$\begin{cases} \dfrac{dN}{dt} = rN\left(1-\dfrac{N}{kS}\right) - \dfrac{\beta PN^2}{\eta^2 S^2 + N^2}, \\ \dfrac{dS}{dt} = \rho S\left(1-\dfrac{S}{s_{\max}}\right) - \delta N. \end{cases} \tag{1.1}$$

The model was originally proposed by Ludwig et al. [18] for spruce-spruce aphid interactions and provided a qualitative analysis of the insect outbreak system, and Anne Rasmussen et al. [20] reviewed and added to the mathematical properties of this model by putting together a model that investigated the number of equilibrium points and stability of the model, and analyzed the relaxation oscillations and calculated the period of these by using singular regression analysis. The model is reviewed and supplemented with a review of the mathematical properties of the model. The predator-feeder model with Holling II functional reflections describes the interactions between predator and prey, including population growth, environmental carrying capacity limits, and the effects of predatory behavior on population dynamics. By analyzing these equations, the dynamic balance between predators and prey in an ecosystem can be better understood. Researchers have done many fruitful works on this class of models [4, 9]. The article [4] studied an improved Holling type II predator-prey model. A complete analysis of the global behavior of the model is presented and it is shown that the model exhibits a dichotomy similar to that of the classical Holling- II model: the coexisting steady state is globally stable; or it is unstable, and thus there exists a unique, globally stable limit ring. The article [9] studied a stochastic predator-prey model with a Holling II increasing function in the predator. The uniqueness of the existence of a global positive solution is proved using Lyapunov analysis. The existence of a smooth distribution in the model, which implies stochastic persistence of predators and prey, is proved. In this paper, the relationship between spruce and budworm larvae is portrayed using a model (1.2) in which the predator has a Holling II functional reflection.

The initial model for the spruce aphids is

$$\begin{cases} \dfrac{dN}{dt} = rN\left(1-\dfrac{N}{kS}\right) - \dfrac{\beta N}{\eta S + N}, \\ \dfrac{dS}{dt} = \rho S\left(1-\dfrac{S}{s_{\max}}\right) - \delta SN, \end{cases} \tag{1.2}$$

where $t$ is the time arrangement, $N$ is bud population density, $S$ is spruce biomass density, $r$ is the intrinsic growth rate of bud population, $\rho$ is the typical growth rate of biomass population,

$k$ is the larval effective bearing coefficient, $S_{\max}$ is the bearing capacity of leaf area, $\beta$ is the maximum consumption of each bud predator, $\delta$ is the average spruce consumption rate of each aphid.

Since the spruce aphid is a species with obvious intergenerational relationship, the reproduction and growth of each generation have clear time intervals rather than a continuous process. The discrete model can naturally reflect this intergenerational characteristic by dividing the dynamic changes of the population into discrete time steps. This model form is more compatible with the actual reproduction pattern of the population, and can more accurately describe the change rule of the population size between generations. The discrete model can reveal some complex dynamical behaviors in the system, and is relatively simple in mathematical treatment, especially in analyzing the stability of the system and the branching phenomenon. The equation form of the discrete model is usually easier to solve and analyze than the continuous model. Therefore to explore the nature of this model, this paper discretizes the known continuous model:

$$\begin{cases} N_{n+1} = N_n + h\left[rN_n\left(1 - \dfrac{N_n}{kS_n}\right) - \dfrac{\beta N_n}{\eta S_n + N_n}\right], \\ S_{n+1} = S_n + h\left[\rho S_n\left(1 - \dfrac{S_n}{S_{\max}}\right) - \delta S_n N_n\right], \end{cases} \tag{1.3}$$

where $h$ represents the step size and has a $h > 0$.

## 2. Existence and stability of the equilibrium points

Now, we discuss the existence of equilibrium of the system (1.3).

(i) The system has a trivial equilibrium point $E(0,0)$.

(ii) The system has a boundary equilibrium point $A(0, S_{\max})$.

(iii) If $\begin{cases} \Delta > 0, \\ N_0 N_1 < 0, \end{cases}$ there is a unique positive equilibrium point $B(N_0, S_0)$, where $N_0 = \frac{((r\eta - rk)S_{\max} - \beta km + 2rk\eta m S_{\max}) + \sqrt{\Delta}}{2((r\eta - rk)m - r + rk\eta m^2)}$, $\Delta = (rk + r\eta)^2 {S_{\max}}^2 + (\beta km + r\eta S_{\max})^2 - r^2\eta^2 {S_{\max}}^2 - 2rk^2 m\beta \times S_{\max} - 4r\beta k S_{\max}$, $N_0 N_1 = \frac{\left(rk\eta {S_{\max}}^2 - \beta k S_{\max}\right)}{((r\eta - rk)m - r + rk\eta m^2)}$.

The Jacmatrix of the system (1.3) is

$$J|_{(N^*,S^*)} = \begin{pmatrix} J_{11}(N^*,S^*) & J_{12}(N^*,S^*) \\ J_{21}(N^*,S^*) & J_{22}(N^*,S^*) \end{pmatrix}, \tag{2.1}$$

$$\begin{aligned} J_{11}(N^*,S^*) &= 1 + hr - \frac{2rhN_n}{kS_n} - \frac{h\beta\eta S_n}{(\eta S_n + N_n)^2}, \\ J_{12}(N^*,S^*) &= \frac{rh{N_n}^2}{k{S_n}^2} + \frac{h\beta\eta N_n}{(\eta S_n + N_n)^2}, \\ J_{21}(N^*,S^*) &= -h\delta S_n, \\ J_{22}(N^*,S^*) &= 1 + h\rho - \frac{2h\rho S_n}{S_{\max}} - h\delta N_n. \end{aligned}$$

The stability of the model (1.3) is discussed below:

**Theorem 2.1.** *For the trivial equilibrium point $E(0,0)$, linear system of (2.1), there are two eigenvalues at $E(0,0)$:*

$$\lambda_1 = 1 + hr, \lambda_2 = 1 + h\rho.$$

*(i) The parameters are all positive, then $E(0,0)$ is a source.*

**Proof.** For the trivial equilibrium point $E(0,0)$,

$$J|_{(E)} = \begin{pmatrix} 1+hr & 0 \\ 0 & 1+h\rho \end{pmatrix},$$

two eigenvalues of the matrix are: $\begin{cases} \lambda_1 = 1 + hr, \\ \lambda_2 = 1 + h\rho. \end{cases}$

(i) $|\lambda_1| > 1$, $|\lambda_2| > 1$, then $E(0,0)$ is a source. □

**Theorem 2.2.** *For the boundary equilibrium point $A(0, S_{\max})$, linear system of (2.1), the characteristic equation at $A(0, S_{\max})$ has two eigenvalues:*

$$\lambda_1 = 1 + hr - \frac{h\beta}{\eta S_{\max}}, \ \lambda_2 = 1 - h\rho.$$

*(i) When* $\begin{cases} 1 - J_{11}(A) J_{22}(A) > 0, \\ 1 + (J_{11}(A) + J_{22}(A)) + J_{11}(A) J_{22}(A) > 0, \\ 1 - (J_{11}(A) + J_{22}(A)) + J_{11}(A) J_{22}(A) > 0, \end{cases}$ *$A(0, S_{\max})$ is a sink.*

*(ii) When* $\begin{cases} 1 + (J_{11}(A) + J_{22}(A)) + J_{11}(A) J_{22}(A) = 0, \\ |J_{11}(A) + J_{22}(A) + 1| < 1, \end{cases}$ *and* $(J_{11}(A) + J_{22}(A))^2 - 4J_{11}(A) \times J_{22}(A) > 0$*, the Flip bifurcation appears at this time.*

*(iii) When* $\begin{cases} 1 - (J_{11}(A) + J_{22}(A)) + J_{11}(A) J_{22}(A) = 0, \\ |J_{11}(A) J_{22}(A) - 1| < 1, \end{cases}$ *and* $(J_{11}(A) + J_{22}(A))^2 - 4J_{11}(A) \times J_{22}(A) > 0$*, the Fold bifurcation occurs at this time.*

*(iv) When $\lambda_1+\lambda_2=J_{11}(A) + J_{22}(A)$, $\lambda_1\lambda_2=J_{11}(A) J_{22}(A)$, $\lambda_1$ and $\lambda_2$ are a pair of conjugated complex roots, the Hopf bifurcation appears.*

**Proof.** For the boundary equilibrium point $A(0, S_{\max})$, $J|_{(A)} = \begin{pmatrix} J_{11}(A) & J_{12}(A) \\ J_{21}(A) & J_{22}(A) \end{pmatrix}$,

$$\begin{aligned} J_{11}(A) &= 1 + hr - \frac{h\beta}{\eta S_{\max}}, \\ J_{12}(A) &= 0, \\ J_{21}(A) &= -h\delta S_{\max}, \\ J_{22}(A) &= 1 - h\rho. \end{aligned}$$

The characteristic equations of the matrix are as:

$$\lambda^2 - (J_{11}(A) + J_{22}(A))\lambda + J_{11}(A) J_{22}(A) = 0,$$

two eigenvalues of the matrix are:

$$\begin{cases} J_{11}(A) = \lambda_1 = 1 + hr - \dfrac{h\beta}{\eta S_{\max}}, \\ J_{22}(A) = \lambda_2 = 1 - h\rho. \end{cases}$$

(i) If $|\lambda_1| < 1$, $|\lambda_2| < 1$, then $\begin{cases} 1 - J_{11}(A) J_{22}(A) > 0, \\ 1 + (J_{11}(A) + J_{22}(A)) + J_{11}(A) J_{22}(A) > 0, \\ 1 - (J_{11}(A) + J_{22}(A)) + J_{11}(A) J_{22}(A) > 0, \end{cases}$ $A(0, S_{\max})$ is a sink.

(ii) If $(J_{11}(A) + J_{22}(A))^2 - 4J_{11}(A) J_{22}(A) > 0$, $\lambda_1 = -1$, $|\lambda_2| < 1$ or $\lambda_2 = -1$, $|\lambda_1| < 1$, then $\begin{cases} 1 + (J_{11}(A) + J_{22}(A)) + J_{11}(A) J_{22}(A) = 0, \\ |J_{11}(A) + J_{22}(A) + 1| < 1, \end{cases}$ the Flip bifurcation appears.

(iii) If $(J_{11}(A) + J_{22}(A))^2 - 4J_{11}(A) J_{22}(A) > 0$, $\lambda_1 = 1$, $|\lambda_2| < 1$ or $\lambda_2 = 1$, $|\lambda_1| < 1$, then $\begin{cases} 1 - (J_{11}(A) + J_{22}(A)) + J_{11}(A) J_{22}(A) = 0, \\ |J_{11}(A) J_{22}(A) - 1| < 1, \end{cases}$ the Fold bifurcation appears.

(iv) If $\lambda_1$ and $\lambda_2$ are a pair of conjugated complex roots, assume $\lambda_1 = a + bi$, $\lambda_2 = a - bi$ $\left(a^2 + b^2 = 1, b \neq 0\right)$, since $(\lambda - \lambda_1)(\lambda - \lambda_2) = \lambda^2 - (\lambda_1 + \lambda_2)\lambda + \lambda_1\lambda_2 = 0$, apparently $\lambda_1+\lambda_2=J_{11}(A) + J_{22}(A)$, $\lambda_1\lambda_2=J_{11}(A) J_{22}(A)$, the Hopf bifurcation appears at this time. □

**Theorem 2.3.** *For the equilibrium point $B(N_0, S_0)$, linear system of* (2.1)*, the characteristic equation at $B(N_0, S_0)$ has two eigenvalues:*

$$\lambda_1 = \frac{J_{11}(B) + J_{22}(B) + \sqrt{(J_{11}(B) + J_{22}(B))^2 - 4(J_{11}(B) J_{22}(B) - J_{12}(B) J_{21}(B))}}{2},$$

$$\lambda_2 = \frac{J_{11}(B) + J_{22}(B) - \sqrt{(J_{11}(B) + J_{22}(B))^2 - 4(J_{11}(B) J_{22}(B) - J_{12}(B) J_{21}(B))}}{2}.$$

*(i) If* $\begin{cases} 1 - J_{11}(B) - J_{22}(B) + J_{11}(B) J_{22}(B) - J_{12}(B) J_{21}(B) > 0, \\ 1 + J_{11}(B) + J_{22}(B) + J_{11}(B) J_{22}(B) - J_{12}(B) J_{21}(B) > 0, \\ 1 - J_{11}(B) J_{22}(B) + J_{12}(B) J_{21}(B) > 0, \end{cases}$ *$B(N_0, S_0)$ is a sink.*

*(ii) If* $\begin{cases} 1 + J_{11}(B) + J_{22}(B) + J_{11}(B) J_{22}(B) - J_{12}(B) J_{21}(B) = 0, \\ |J_{11}(B) + J_{22}(B) + 1| < 1, \end{cases}$ *and* $(J_{11}(B) + J_{22}(B))^2 - 4(J_{11}(B) J_{22}(B) - J_{12}(B) J_{21}(B)) > 0$*, the Flip bifurcation appears.*

*(iii) If* $\begin{cases} 1 - J_{11}(B) - J_{22}(B) + J_{11}(B) J_{22}(B) - J_{12}(B) J_{21}(B) = 0, \\ |J_{11}(B) + J_{22}(B) - 1| < 1, \end{cases}$ *and* $(J_{11}(B)+J_{22}(B))^2 - 4(J_{11}(B) J_{22}(B) - J_{12}(B) J_{21}(B))$*, the Fold bifurcation appears.*

*(iv) If $\lambda_1+\lambda_2=J_{11}(B) + J_{22}(B)$, $\lambda_1\lambda_2=J_{11}(B) J_{22}(B) - J_{12}(B) J_{21}(B)$, $\lambda_1$ and $\lambda_2$ are a pair of conjugated complex roots, the Hopf bifurcation appears.*

**Proof.** For the equilibrium point $B(N_0, S_0)$, $J|_{(B)} = \begin{pmatrix} J_{11}(B) & J_{12}(B) \\ J_{21}(B) & J_{22}(B) \end{pmatrix}$,

$$J_{11}(B) = 1 + hr - \frac{2r\rho th}{kS_{\max}(\rho l - \delta t)} - \frac{h\beta\eta S_{\max}(\rho l - \delta t)}{\rho l\left(\eta S_{\max}\left(1 - \frac{\delta t}{\rho l}\right) + \frac{t}{l}\right)^2},$$

$$J_{12}(B) = \frac{hrt^2}{kl^2\left(S_{\max}\left(1 - \frac{\delta t}{\rho l}\right)\right)^2} + \frac{h\beta\eta t}{l\left(\eta S_{\max}\left(1 - \frac{\delta t}{\rho l}\right) + \frac{t}{l}\right)^2},$$

$$J_{21}(B) = -h\delta\left(\left(1 - \frac{\delta t}{\rho l}\right)\right) S_{\max},$$

$$J_{22}(B) = 1 - h\rho + \frac{h\delta t}{l}.$$

The characteristic equations of the matrix are as:

$$\lambda^2 - (J_{11}(B) + J_{22}(B))\lambda + J_{11}(B) J_{22}(B) - J_{12}(B) J_{21}(B) = 0,$$

the two characteristic values of the array are:

$$\begin{cases} \lambda_1 = \dfrac{J_{11}(B) + J_{22}(B) + \sqrt{(J_{11}(B) + J_{22}(B))^2 - 4(J_{11}(B) J_{22}(B) - J_{12}(B) J_{21}(B))}}{2}, \\ \lambda_2 = \dfrac{J_{11}(B) + J_{22}(B) - \sqrt{(J_{11}(B) + J_{22}(B))^2 - 4(J_{11}(B) J_{22}(B) - J_{12}(B) J_{21}(B))}}{2}. \end{cases}$$

(i) If $|\lambda_1| < 1$, $|\lambda_2| < 1$,

then $\begin{cases} 1 - J_{11}(B) - J_{22}(B) + J_{11}(B) J_{22}(B) - J_{12}(B) J_{21}(B) > 0, \\ 1 + J_{11}(B) + J_{22}(B) + J_{11}(B) J_{22}(B) - J_{12}(B) J_{21}(B) > 0, \\ 1 - J_{11}(B) J_{22}(B) + J_{12}(B) J_{21}(B) > 0, \end{cases}$ $B(N_0, S_0)$ is a sink.

(ii) If $(J_{11}(B) + J_{22}(B))^2 - 4(J_{11}(B) J_{22}(B) - J_{12}(B) J_{21}(B)) > 0$, $\lambda_1 = -1$, $|\lambda_2| < 1$ or $\lambda_2 = -1$, $|\lambda_1| < 1$,

then $\begin{cases} 1 + J_{11}(B) + J_{22}(B) + J_{11}(B) J_{22}(B) - J_{12}(B) J_{21}(B) = 0, \\ |J_{11}(B) + J_{22}(B) + 1| < 1, \end{cases}$ the Flip bifurcation appears at this time.

(iii) If $(J_{11}(B) + J_{22}(B))^2 - 4(J_{11}(B) J_{22}(B) - J_{12}(B) J_{21}(B)) > 0$, $\lambda_1 = 1$, $|\lambda_2| < 1$ or $\lambda_2 = 1$, $|\lambda_1| < 1$,

then $\begin{cases} 1 - J_{11}(B) - J_{22}(B) + J_{11}(B) J_{22}(B) - J_{12}(B) J_{21}(B) = 0, \\ |J_{11}(B) + J_{22}(B) - 1| < 1, \end{cases}$ the Fold bifurcation appears at this time.

(iv) If $\lambda_1$ and $\lambda_2$ are a pair of conjugated complex roots, assume $\lambda_1 = a + bi$, $\lambda_2 = a - bi$ $\left(a^2 + b^2 = 1, b \neq 0\right)$, since $(\lambda - \lambda_1)(\lambda - \lambda_2) = \lambda^2 - (\lambda_1 + \lambda_2)\lambda + \lambda_1\lambda_2 = 0$, apparently $\lambda_1 + \lambda_2 = J_{11}(B) + J_{22}(B)$, $\lambda_1\lambda_2 = J_{11}(B) J_{22}(B) - J_{12}(B) J_{21}(B)$, the Hopf bifurcation appears at this time. □

# 3. Flip bifurcation at positive equilibrium point

## 3.1. The existence conditions of Flip bifurcation

Suppose that the $t = ((r\eta - rk)\, S_{\max} - \beta km + 2rk\eta m S_{\max}) + \sqrt{\Delta}$, $\Delta = (rk + r\eta)^2 {S_{\max}}^2 + (\beta km + r\eta S_{\max})^2 - r^2\eta^2 {S_{\max}}^2 - 2rk^2 m\beta S_{\max} - 4r\beta k S_{\max}$, $l = 2\left((r\eta - rk)\, m - r + rk\eta m^2\right)$, then $N_0 = \frac{t}{l}$, $S_0 = \left(1 - \frac{\delta t}{\rho l}\right)$, $Z = \left(r - \frac{2r\rho t}{kS_{\max}(\rho l - \delta t)} - \frac{\beta\eta S_{\max}(\rho l - \delta t)}{\rho l\left(\eta S_{\max}\left(1 - \frac{\delta t}{\rho l}\right) + \frac{t}{l}\right)^2}\right)$, $M = \frac{rt^2}{kl^2\left(S_{\max}\left(1 - \frac{\delta t}{\rho l}\right)\right)^2} + \frac{\beta\eta t}{l\left(\eta S_{\max}\left(1 - \frac{\delta t}{\rho l}\right) + \frac{t}{l}\right)^2}$.

At this point $B(N_0, S_0)$ the Jacbian is:

$$J(B) = \begin{pmatrix} 1 + hZ & hM \\ -h\delta\left(\left(1 - \dfrac{\delta t}{\rho l}\right)\right) S_{\max} & 1 - h\rho + \dfrac{h\delta t}{l} \end{pmatrix},$$

in order to obtain the bifurcation arguments, think about the transformation $\overline{N_{n+1}} = N_{n+1} - N_0$, $\overline{S_{n+1}} = S_{n+1} - S_0$ to move $N_0$, $S_0$ to the origin, and (1.3) can be formulated as:

$$\begin{cases} \overline{N_{n+1}} = \overline{N_n} + h\left[r\left(\overline{N_n} + N_0\right)\left(1 - \dfrac{\left(\overline{N_n} + N_0\right)}{k\left(\overline{S_n} + S_0\right)}\right) - \dfrac{\beta\left(\overline{N_n} + N_0\right)}{\eta\left(\overline{S_n} + S_0\right) + \left(\overline{N_n} + N_0\right)}\right], \\ \overline{S_{n+1}} = \overline{S_n} + h\left[\rho\left(\overline{S_n} + S_0\right)\left(1 - \dfrac{\left(\overline{S_n} + S_0\right)}{S_{\max}}\right) - \delta\left(\overline{S_n} + S_0\right)\left(\overline{N_n} + N_0\right)\right], \end{cases} \tag{3.1}$$

equation (3.1) uses a Taylor expansion at $B(N_0, S_0)$ to obtain the following expression:

$$\begin{pmatrix} \overline{N_{n+1}} \\ \overline{S_{n+1}} \end{pmatrix} = J|_{(N_0, S_0)} \begin{pmatrix} \overline{N_n} \\ \overline{S_n} \end{pmatrix} + h \begin{pmatrix} \psi_1\left(\overline{N_n}, \overline{S_n}\right) \\ \psi_2\left(\overline{N_n}, \overline{S_n}\right) \end{pmatrix}, \tag{3.2}$$

where

$$\begin{aligned} \psi_1\left(\overline{N_n}, \overline{S_n}\right) =& z_1\overline{N_n}^2 + z_2\overline{N_n S_n} + z_3\overline{S_n}^2 + z_4\overline{N_n}^3 + z_5\overline{N_n}^2\overline{S_n} + z_6\overline{N_n S_n}^2 + z_7\overline{S_n}^3 \\ & + O\left(\left(\left|\overline{N_n}\right| + \left|\overline{S_n}\right|\right)^4\right), \\ \psi_2\left(\overline{N_n}, \overline{S_n}\right) =& u_1\overline{N_n S_n} + u_2\overline{S_n}^2 + O\left(\left(\left|\overline{N_n}\right| + \left|\overline{S_n}\right|\right)^4\right), \\ z_1 =& -\frac{r}{kS_0} + \frac{\beta\eta S_0}{(\eta S_0 + N_0)^3}, \\ z_2 =& \frac{rN_0}{k{S_0}^2} + \frac{\beta\eta^2 S_0 - \beta\eta N_0}{2(\eta S_0 + N_0)^3}, \\ z_3 =& -\frac{r{N_0}^2}{k{S_0}^3} - \frac{\beta\eta^2 N_0}{(\eta S_0 + N_0)^3},\ z_4 = -\frac{\beta\eta S_0}{(\eta S_0 + N_0)^4}, \\ z_5 =& \frac{r}{3k{S_0}^2} + \frac{\beta\eta N_0 - 2\beta\eta^2 S_0}{3(\eta S_0 + N_0)^4}, \\ z_6 =& -\frac{2rN_0}{3k{S_0}^3} + \frac{2\beta\eta^2 N_0 - \beta\eta^3 S_0}{3(\eta S_0 + N_0)^4}, \end{aligned}$$

$z_7 = \dfrac{rN_0{}^2}{kS_0{}^4} + \dfrac{\beta\eta^3 N_0}{(\eta S_0 + N_0)^4}$, $u_1 = -\dfrac{\delta}{2}$, $u_2 = -\dfrac{\rho}{S_{\max}}$.

On the basis of the characteristic polynomial, it can be obtained:

$$f(-1) = \left(Z\left(\frac{\delta t}{l} - \rho\right) + M\left(\delta S_{\max}\left(1 - \frac{\delta t}{\rho l}\right)\right)\right)h^2 + 2\left(Z + \frac{\delta t}{l} - \rho\right)h + 4,$$

solution to $h^* = \frac{-d_2 + \sqrt{d_2{}^2 - 16d_1}}{2d_1}$, where $d_1 = Z\left(\frac{\delta t}{l} - \rho\right) + M\delta S_{\max}\left(1 - \frac{\delta t}{\rho l}\right)$, $d_2 = 2\left(Z + \frac{\delta t}{l} - \rho\right)$.

Consider the parameter $h$ with a small perturbation $\delta_0$, then $h = h^* + \delta_0$, $|\delta_0| \ll 2$, and the system (3.2) changes to:

$$\begin{aligned}\begin{pmatrix}\overline{N_{n+1}}\\ \overline{S_{n+1}}\end{pmatrix} = &\begin{pmatrix}1 + (h^* + \delta_0)Z & (h^* + \delta_0)M\\ -(h^* + \delta_0)\left(\delta S_{\max}\left(1 - \dfrac{\delta t}{\rho l}\right)\right) & 1 + (h^* + \delta_0)\left(\dfrac{\delta t}{l} - \rho\right)\end{pmatrix}\begin{pmatrix}\overline{N_n}\\ \overline{S_n}\end{pmatrix}\\ &+ (h^* + \delta_0)\begin{pmatrix}\psi_1\left(\overline{N_n}, \overline{S_n}\right)\\ \psi_2\left(\overline{N_n}, \overline{S_n}\right)\end{pmatrix},\end{aligned} \tag{3.3}$$

the characteristic polynomial of the above formula is:

$$\begin{aligned}g(\lambda) =& \lambda^2 - \left(2 + (h^* + \delta_0)\left(Z + \frac{\delta t}{l} - \rho\right)\right)\lambda + (1 + (h^* + \delta_0)Z)\left(1 + (h^* + \delta_0)\left(\frac{\delta t}{l} - \rho\right)\right)\\ &+ (h^* + \delta_0)^2 M\delta S_{\max}\left(1 - \frac{\delta t}{\rho l}\right),\end{aligned}$$

the transversal condition at $B(N_0, S_0)$ is given by:

$$\begin{aligned}\left.\frac{dg(\lambda)}{d\delta_0}\right|_{\lambda=-1,\delta_0=0} =& \left(Z + \frac{\delta t}{l} - \rho\right) + Z\left(1 + h^*\left(\frac{\delta t}{l} - \rho\right)\right) + \left((1 + h^* Z)\left(\frac{\delta t}{l} - \rho\right)\right)\\ &+ Mh^*\delta S_{\max}\left(1 - \frac{\delta t}{\rho l}\right) + h^* M\delta S_{\max}\left(1 - \frac{\delta t}{\rho l}\right).\end{aligned}$$

### 3.2. The canonical form of Flip bifurcation solutions

For discussion convenience, defined

$$A = \begin{pmatrix}1 + h^* Z & h^* M\\ -h^*\left(\delta S_{\max}\left(1 - \dfrac{\delta t}{\rho l}\right)\right) & 1 + h^*\left(\dfrac{\delta t}{l} - \rho\right)\end{pmatrix},$$

if the characteristic value of $A$ is $\lambda = \lambda_1 = -1$, the corresponding feature vector is:

$$T_1 = \begin{pmatrix}h^* M\\ -2 - h^* Z\end{pmatrix},$$

if the characteristic value of $A$ is $\lambda = \lambda_2$, the corresponding feature vector is:

$$T_2 = \begin{pmatrix}h^* M\\ \lambda_2 - 1 - h^* Z\end{pmatrix},$$

as follows reversible matrix can be acquired:

$$T = \begin{pmatrix} T_1 \, T_2 \end{pmatrix} = \begin{pmatrix} h^*M & h^*M \\ -2 - h^*Z & \lambda_2 - 1 - h^*Z \end{pmatrix},$$

let

$$\begin{pmatrix} X_{n+1} \\ Y_{n+1} \end{pmatrix} = T^{-1} \begin{pmatrix} \overline{N_{n+1}} \\ \overline{S_{n+1}} \end{pmatrix},$$

then

$$\begin{pmatrix} X_n \\ Y_n \end{pmatrix} = T^{-1} \begin{pmatrix} \overline{N_n} \\ \overline{S_n} \end{pmatrix},$$

that is:

$$\begin{pmatrix} X_{n+1} \\ Y_{n+1} \end{pmatrix} = \begin{pmatrix} -1 & 0 \\ 0 & \lambda_2 \end{pmatrix} \begin{pmatrix} X_n \\ Y_n \end{pmatrix} + \begin{pmatrix} f_1\left(\overline{N_n}, \overline{S_n}, \delta_0\right) \\ f_2\left(\overline{N_n}, \overline{S_n}, \delta_0\right) \end{pmatrix}, \tag{3.4}$$

where

$$\begin{aligned} f_1\left(\overline{N_n}, \overline{S_n}, \delta_0\right) =& a_{11}\overline{N_n}\delta_0 + a_{12}\overline{S_n}\delta_0 + b_{11}\overline{N_n}^2 + b_{12}\overline{N_n S_n} + b_{13}\overline{S_n}^2 + b_{14}\overline{N_n}^3 \\ &+ b_{15}\overline{N_n}^2\overline{S_n} + b_{16}\overline{N_n S_n}^2 + b_{17}\overline{S_n}^3, \\ f_2\left(\overline{N_n}, \overline{S_n}, \delta_0\right) =& a_{21}\overline{N_n}\delta_0 + a_{22}\overline{S_n}\delta_0 + b_{21}\overline{N_n}^2 + b_{22}\overline{N_n S_n} + b_{23}\overline{S_n}^2 + b_{24}\overline{N_n}^3 \\ &+ b_{25}\overline{N_n}^2\overline{S_n} + b_{26}\overline{N_n S_n}^2 + b_{27}\overline{S_n}^3, \end{aligned}$$

$$a_{11} = \left(\frac{\lambda_2 - 1 - h^*Z}{h^*M\left(\lambda_2 + 1\right)}\right) Z + \frac{\delta S_{\max}\left(1 - \frac{\delta t}{\rho l}\right)}{\left(\lambda_2 + 1\right)},$$

$$a_{12} = \left(\frac{\lambda_2 - 1 - h^*Z}{h^*\left(\lambda_2 + 1\right)}\right) - \frac{\frac{\delta t}{l} - \rho}{\left(\lambda_2 + 1\right)},$$

$$a_{21} = -\left(\frac{2 + h^*Z}{h^*M\left(\lambda_2 + 1\right)}\right) Z - \frac{\delta S_{\max}\left(1 - \frac{\delta t}{\rho l}\right)}{\left(\lambda_2 + 1\right)},$$

$$a_{22} = \left(\frac{2 + h^*Z}{h^*\left(\lambda_2 + 1\right)}\right) + \frac{\frac{\delta t}{l} - \rho}{\left(\lambda_2 + 1\right)},$$

$$b_{11} = \left(\frac{\lambda_2 - 1 - h^*Z}{M\left(\lambda_2 + 1\right)}\right) z_1,\ b_{12} = \left(\frac{\lambda_2 - 1 - h^*Z}{M\left(\lambda_2 + 1\right)}\right) z_2 - \frac{u_1 h^*}{\left(\lambda_2 + 1\right)},$$

$$b_{13} = \left(\frac{\lambda_2 - 1 - h^*Z}{M\left(\lambda_2 + 1\right)}\right) z_3 - \frac{u_2 h^*}{\left(\lambda_2 + 1\right)},\ b_{14} = \left(\frac{\lambda_2 - 1 - h^*Z}{M\left(\lambda_2 + 1\right)}\right) z_4,$$

$$b_{15} = \left(\frac{\lambda_2 - 1 - h^*Z}{M\left(\lambda_2 + 1\right)}\right) z_5,\ b_{16} = \left(\frac{\lambda_2 - 1 - h^*Z}{M\left(\lambda_2 + 1\right)}\right) z_6,$$

$$b_{17} = \left(\frac{\lambda_2 - 1 - h^*Z}{M\left(\lambda_2 + 1\right)}\right) z_7,\ b_{21} = \left(\frac{2 + h^*Z}{M\left(\lambda_2 + 1\right)}\right) z_1,$$

$$b_{22} = \left(\frac{2 + h^*Z}{M\left(\lambda_2 + 1\right)}\right) z_2 + \frac{u_1 h^*}{\left(\lambda_2 + 1\right)},$$

$$b_{23}=\left(\frac{2+h^*Z}{M\left(\lambda_2+1\right)}\right)z_3+\frac{u_2h^*}{(\lambda_2+1)},$$
$$b_{24}=\left(\frac{2+h^*Z}{M\left(\lambda_2+1\right)}\right)z_4,\ b_{25}=\left(\frac{2+h^*Z}{M\left(\lambda_2+1\right)}\right)z_5,$$
$$b_{26}=\left(\frac{2+h^*Z}{M\left(\lambda_2+1\right)}\right)z_6,\ b_{27}=\left(\frac{2+h^*Z}{M\left(\lambda_2+1\right)}\right)z_7.$$

From

$$\begin{pmatrix}X_n\\Y_n\end{pmatrix}=T^{-1}\begin{pmatrix}\overline{N_n}\\\overline{S_n}\end{pmatrix},$$

then

$$\begin{pmatrix}\overline{N_n}\\\overline{S_n}\end{pmatrix}=T\begin{pmatrix}X_n\\Y_n\end{pmatrix}=\begin{pmatrix}h^*M & h^*M\\-2-h^*Z & \lambda_2-1-h^*Z\end{pmatrix}\begin{pmatrix}X_n\\Y_n\end{pmatrix},$$

and

$$\overline{N_n}=h^*M\left(X_n+Y_n\right),\overline{S_n}=\left(-2-h^*Z\right)X_n+\left(\lambda_2-1-h^*Z\right)Y_n,$$

by substituting (3.4), it can be concluded that:

$$\begin{pmatrix}X_{n+1}\\Y_{n+1}\end{pmatrix}=\begin{pmatrix}-X_n\\\lambda_2Y_n\end{pmatrix}+\begin{pmatrix}f_3\left(X_n,Y_n,\delta_0\right)\\f_4\left(X_n,Y_n,\delta_0\right)\end{pmatrix},\tag{3.5}$$
$$\begin{aligned}f_3\left(X_n,Y_n,\delta_0\right)=&d_{11}X_n\delta_0+d_{12}Y_n\delta_0+e_{11}{X_n}^2+e_{12}X_nY_n+e_{13}{Y_n}^2+e_{14}{X_n}^3\\&+e_{15}{X_n}^2Y_n+e_{16}X_n{Y_n}^2+e_{17}{Y_n}^3,\\f_4\left(X_n,Y_n,\delta_0\right)=&d_{21}X_n\delta_0+d_{22}Y_n\delta_0+e_{21}{X_n}^2+e_{22}X_nY_n+e_{23}{Y_n}^2+e_{24}{X_n}^3\\&+e_{25}{X_n}^2Y_n+e_{26}X_n{Y_n}^2+e_{27}{Y_n}^3\end{aligned}$$

let $k_{11}=k_{12}=h^*M$, $k_{21}=(-2-h^*Z)$, $k_{22}=(\lambda_2-1-h^*Z)$, where

$$\begin{aligned}d_{11}&=a_{11}k_{11}+a_{12}k_{21},\\d_{12}&=a_{11}k_{12}+a_{12}k_{22},\\e_{11}&=b_{11}{k_{11}}^2+b_{12}k_{11}k_{21}+b_{13}{k_{21}}^2,\\e_{12}&=2b_{11}k_{11}k_{12}+b_{12}\left(k_{11}k_{22}+k_{12}k_{21}\right)+2b_{13}k_{21}k_{22},\\e_{13}&=b_{11}{k_{12}}^2+b_{12}k_{12}k_{22}+b_{13}{k_{22}}^2,\\e_{14}&=b_{14}{k_{11}}^3+b_{15}{k_{11}}^2k_{21}+b_{16}{k_{21}}^2k_{11}+b_{17}{k_{21}}^3,\\e_{15}&=3b_{14}{k_{11}}^2k_{12}+b_{15}\left(2k_{11}k_{12}k_{21}+{k_{11}}^2k_{22}\right)+b_{16}\left(2k_{11}k_{22}k_{21}+{k_{21}}^2k_{12}\right)\\&\quad+3b_{17}{k_{21}}^2k_{22},\\e_{16}&=3b_{14}{k_{12}}^2k_{11}+b_{15}\left(2k_{11}k_{12}k_{22}+{k_{12}}^2k_{21}\right)+b_{16}\left(2k_{12}k_{22}k_{21}+{k_{22}}^2k_{11}\right)\\&\quad+3b_{17}{k_{22}}^2k_{21},\\e_{17}&=b_{14}{k_{12}}^3+b_{15}{k_{12}}^2k_{22}+b_{16}{k_{22}}^2k_{12}+b_{17}{k_{22}}^3,\\d_{21}&=a_{21}k_{11}+a_{22}k_{21},\\d_{22}&=a_{21}k_{12}+a_{22}k_{22},\\e_{21}&=b_{21}{k_{11}}^2+b_{22}k_{11}k_{21}+b_{23}{k_{21}}^2,\\e_{22}&=2b_{21}k_{11}k_{12}+b_{22}\left(k_{11}k_{22}+k_{12}k_{21}\right)+2b_{23}k_{21}k_{22},\\e_{23}&=b_{21}{k_{12}}^2+b_{22}k_{12}k_{22}+b_{23}{k_{22}}^2,\end{aligned}$$

$$
\begin{aligned}
e_{24} &= b_{24}{k_{11}}^3 + b_{25}{k_{11}}^2 k_{21} + b_{26}{k_{21}}^2 k_{11} + b_{27}{k_{21}}^3,\\
e_{25} &= 3b_{24}{k_{11}}^2 k_{12} + b_{25}\left(2k_{11}k_{12}k_{21} + {k_{11}}^2 k_{22}\right) + b_{26}\left(2k_{11}k_{22}k_{21} + {k_{21}}^2 k_{12}\right)\\
&\quad + 3b_{27}{k_{21}}^2 k_{22},\\
e_{26} &= 3b_{24}{k_{12}}^2 k_{11} + b_{25}\left(2k_{11}k_{12}k_{22} + {k_{12}}^2 k_{21}\right) + b_{26}\left(2k_{12}k_{22}k_{21} + {k_{22}}^2 k_{11}\right)\\
&\quad + 3b_{27}{k_{22}}^2 k_{21},\\
e_{27} &= b_{24}{k_{12}}^3 + b_{25}{k_{12}}^2 k_{22} + b_{26}{k_{22}}^2 k_{12} + b_{27}{k_{22}}^3,\\
e_{ij} &= h^* f_{ij} (i = 1, 2; j = 1, 2, \cdots, 7).
\end{aligned}
$$

The following discusses the direction of the Flip bifurcation at $B\left(N_0, S_0\right)$, using the central manifold theorem and the gauge theory:

$$
\begin{aligned}
\theta_1 &= \left(\frac{\partial^2 f}{\partial X_n \partial \delta_0} + \frac{1}{2}\frac{\partial f}{\partial \delta_0}\frac{\partial^2 f}{\partial {X_n}^2}\right)\Bigg|_{(0,0)},\\
\theta_2 &= \left(\frac{1}{6}\frac{\partial^3 f}{\partial {X_n}^3} + \left(\frac{1}{2}\frac{\partial^2 f}{\partial {X_n}^2}\right)^2\right)\Bigg|_{(0,0)}.
\end{aligned}
$$

**Theorem 3.1.** *If $\theta_1 \neq 0$,$\theta_2 \neq 0$, the system has a Flip bifurcation at the fixed point $B\left(N_0, S_0\right)$, and if $\theta_2 > 0 (\theta_2 < 0)$, the point of period 2 is stable (unstable).*

**Proof.** For a adequate small neighborhood at the argument $\delta_0 = 0$, there is a central manifold at $(0, 0)$:

$$
W^c = \left\{(X_n, Y_n) : Y_n = m_1 {X_n}^2 + m_2 X_n \delta_0\right\}, \tag{3.6}
$$

put (3.5) into (3.4):

$$
Y_{n+1} = m_1 {X_{n+1}}^2 + m_2 X_{n+1}\delta_0, \text{ then } Y_n = m_1 {X_n}^2 + m_2 X_n \delta_0,
$$

then

$$
\begin{aligned}
&X_{n+1} \approx e_{11}{X_n}^2 + \left(-1 + d_{11}\delta_0\right) X_n,\\
&X_{n+1}\delta_0 \approx -X_n \delta_0,\\
&{X_{n+1}}^2 = {X_n}^2,\\
&Y_{n+1} = \left(\lambda_1 m_1 + e_{21}\right){X_n}^2 + \left(\lambda_1 m_2 + d_{21}\right) X_n \delta_0 = m_1 {X_{n+1}}^2 + m_2 X_{n+1}\delta_0,\\
&m_1 = \frac{e_{21}}{1 - \lambda_2} = \frac{b_{21}{k_{11}}^2 + b_{22}k_{11}k_{21} + b_{23}{k_{21}}^2}{1 - \lambda_2},\\
&m_2 = \frac{-d_{21}}{1 + \lambda_2} = \frac{-\left(a_{21}k_{11} + a_{22}k_{21}\right)}{1 + \lambda_2},
\end{aligned}
$$

limit the equations to $W^c\left(0, 0\right)$ with the following results:

$$
\begin{aligned}
X_{n+1} = &- X_n + e_{11}{X_n}^2 + d_{11}X_n\delta_0 + \left(d_{12}m_1 + e_{12}m_2\right){X_n}^2\delta_0 + \left(e_{12}m_1 + e_{14}\right){X_n}^3\\
&+ O\left(\left(\left|\overline{N_n}\right| + \left|\overline{S_n}\right|\right)^4\right).
\end{aligned}
$$

According to reference [8], at $(X, Y, \delta_0) = (0, 0, 0)$, if $\theta_1 \neq 0$,$\theta_2 \neq 0$, the system experiences a Flip bifurcation at point $B\left(N_0, S_0\right)$, and if $\theta_2 > 0$, $(\theta_2 < 0)$, the point of period 2 is stable (unstable), where

$$
\theta_1 = \left(\frac{\partial^2 f}{\partial X_n \partial \delta_0} + \frac{1}{2}\frac{\partial f}{\partial \delta_0}\frac{\partial^2 f}{\partial {X_n}^2}\right)\Bigg|_{(0,0)} = d_{11} + d_{12}m_1 + e_{12}m_2,
$$

$$\theta_2 = \left( \frac{1}{6} \frac{\partial^3 f}{\partial {X_n}^3} + \left( \frac{1}{2} \frac{\partial^2 f}{\partial {X_n}^2} \right)^2 \right) \Bigg|_{(0,0)} = e_{12} m_1 + e_{14} + {e_{11}}^2.$$

□

Numerical simulation is used to prove the above results. Now we set $k = 10000$, $\eta = 7.54$, $\beta = 14.96$, $\rho = 0.9$, $h = 0.262122270347572$, $S_{\max} = 50$, $\delta = 0.6$, $r = 10$, $B(N_0, S_0) = (1.499951950752, 0.001601641574)$:

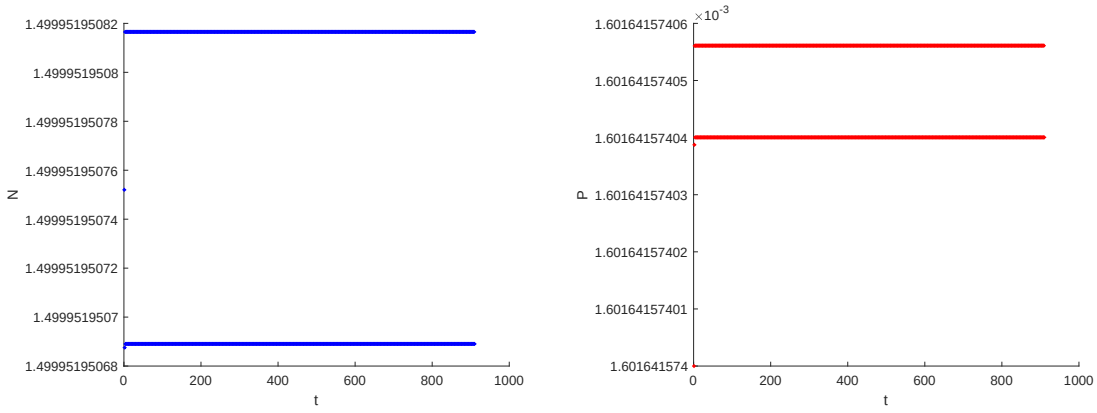


**Figure 1.** The graph of $N$, $S$ when Flip bifurcation occurs at $k = 10000$, $\eta = 7.54$, $\beta = 14.96$, $\rho = 0.9$, $h = 0.262122270347572$, $S_{\max} = 50$, $\delta = 0.6$, $r = 10$, $B(N_0, S_0) = (1.499951950752, 0.001601641574)$.

# 4. Hopf bifurcation at point $B(N_0, S_0)$

## 4.1. The existence conditions of Hopf bifurcation

For the Hopf bifurcation occurring near the positive equilibrium point $B(N_0, S_0)$, the two roots of the characteristic polynomial must be a pair of conjugated unit compound radical. Therefore, the bifurcation parameters are readily obtained:

$$\lambda_1 \lambda_2 = J_{11}(B) J_{22}(B) - J_{12}(B) J_{21}(B) = 1,$$

select the bifurcation parameter as:

$$h^* = -\frac{\left(Z + \frac{\delta t}{l} - \rho\right)}{Z\left(\frac{\delta t}{l} - \rho\right) + M\left(\delta S_{\max}\left(1 - \frac{\delta t}{\rho l}\right)\right)},$$

with $h > 0$, we still consider the parameter $h$ with small perturbations $\delta_0$, namely $h = h^* + \delta_0$, $|\delta_0| \ll 1$, then the characteristic equation can be written as:

$$\lambda^2 + p(\delta_0)\lambda + q(\delta_0) = 0,$$

where

$$p(\delta_0) = -\left(2 + (h^* + \delta_0)\left(Z + \frac{\delta t}{l} - \rho\right)\right),$$

$$q(\delta_0) = 1 + (h^* + \delta_0)\left(Z + \frac{\delta t}{l} - \rho\right) + (h^* + \delta_0)^2\left(Z\left(\frac{\delta t}{l} - \rho\right) + M\delta S_{\max}\left(1 - \frac{\delta t}{\rho l}\right)\right),$$

the root of the equation at $J|_{(N_0,S_0)}$ is

$$\lambda_1 = \frac{p(\delta_0) + i\sqrt{4q(\delta_0) - p(\delta_0)^2}}{2},$$

$$\lambda_2 = \frac{p(\delta_0) - i\sqrt{4q(\delta_0) - p(\delta_0)^2}}{2}, \text{ and } |\lambda_{1,2}| = \sqrt{q(\delta_0)}.$$

$$\begin{aligned}\left.\frac{d|\lambda_{1,2}|}{d\delta_0}\right|_{\delta_0=0} =& \frac{1}{2}\left(\left(Z + \frac{\delta t}{l} - \rho\right) + 2h^*\left(Z\left(\frac{\delta t}{l} - \rho\right) + M\delta S_{\max}\left(1 - \frac{\delta t}{\rho l}\right)\right)\right) \\ &\times \left(1 + h^*\left(Z + \frac{\delta t}{l} - \rho\right) + (h^*)^2\left(Z\left(\frac{\delta t}{l} - \rho\right) + M\delta S_{\max}\left(1 - \frac{\delta t}{\rho l}\right)\right)\right)^{-\frac{1}{2}},\end{aligned}$$

if and only if $\left(Z + \frac{\delta t}{l} - \rho\right) + 2h^*\left(Z\left(\frac{\delta t}{l} - \rho\right) + M\delta S_{\max}\left(1 - \frac{\delta t}{\rho l}\right)\right) > 0$, $\left.\frac{d|\lambda_{1,2}|}{d\delta_0}\right|_{\delta_0=0} > 0$, if $p(0) \neq 0, 1$, then $-(h^* + \delta_0)\left(Z + \frac{\delta t}{l} - \rho\right) \neq 2, 3$, ${\lambda_{1,2}}^n \neq 1$, $n = 1, 2, 3, 4$.

The cross-sectional condition at the positive equilibrium point $B(N_0, S_0)$ is:

$$\begin{aligned}\left.\frac{d|\lambda_{1,2}|}{d\delta_0}\right|_{\delta_0=0} &= \left(\lambda_1\frac{d\lambda_2}{d\delta_0} + \lambda_2\frac{d\lambda_1}{d\delta_0}\right)\Big|_{\delta_0=0} \\ &= \frac{1}{2}(-i-1)h^*iZ - \frac{1}{2}(-i-1)h^*Z - \frac{1}{2}(i-1)h^*Z - \frac{1}{2}(i-1)h^*iZ \\ &= \left(h^* - h^*i^2\right)Z,\end{aligned}$$

when $\left.\frac{d|\lambda_1|^2}{d\delta_0}\right|_{\delta_0=0} > 0$, the Hopf Bifurcation exists at the positive equilibrium point $B(N_0, S_0)$.

### 4.2. The canonical form of Hopf bifurcation solutions

Let

$$u = \frac{1}{2}\left(-\left(2 + h\left(Z + \frac{\delta t}{l} - \rho\right)\right)\right),$$

$$v = \frac{1}{2}h\sqrt{4\left(Z\left(\frac{\delta t}{l} - \rho\right) + M\delta S_{\max}\left(1 - \frac{\delta t}{\rho l}\right)\right) - \left(Z + \frac{\delta t}{l} - \rho\right)^2},$$

the corresponding reof $\lambda_1 = u + iv$ and the $\lambda_2 = u - iv$ are:

$$T = \begin{pmatrix} T_1 & T_2 \end{pmatrix} = \begin{pmatrix} hM & 0 \\ u - 1 - hZ & v \end{pmatrix}, T^{-1} = \begin{pmatrix} \frac{1}{hM} & 0 \\ -\frac{u - 1 - hZ}{hM} & \frac{1}{v} \end{pmatrix},$$

use the following transformation:

$$\begin{pmatrix} \overline{N_{n+1}} \\ \overline{S_{n+1}} \end{pmatrix} = T\begin{pmatrix} \overline{X_{n+1}} \\ \overline{Y_{n+1}} \end{pmatrix},$$

then, equation (3.3) transforms to:

$$\begin{pmatrix} X_{n+1} \\ Y_{n+1} \end{pmatrix} = \begin{pmatrix} u & -v \\ v & u \end{pmatrix} \begin{pmatrix} X_n \\ Y_n \end{pmatrix} + \begin{pmatrix} \widetilde{f}\left(\overline{X_n}, \overline{Y_n}\right) \\ \widetilde{g}\left(\overline{X_n}, \overline{Y_n}\right) \end{pmatrix},$$

where

$$\begin{aligned}
&\widetilde{f}\left(\overline{X_n}, \overline{Y_n}\right) = T^{-1} f\left(\overline{X_n}, \overline{Y_n}\right), \widetilde{g}\left(\overline{X_n}, \overline{Y_n}\right) = T^{-1} g\left(\overline{X_n}, \overline{Y_n}\right), \\
&f\left(\overline{X_n}, \overline{Y_n}\right) = e_1 \overline{X_n}^2 + e_2 \overline{X_n Y_n} + e_3 \overline{Y_n}^2 + e_4 \overline{X_n}^3 + e_5 \overline{X_n}^2 \overline{Y_n} + e_6 \overline{X_n Y_n}^2 + e_7 \overline{Y_n}^3, \\
&g\left(\overline{X_n}, \overline{Y_n}\right) = s_1 \overline{X_n}^2 + s_2 \overline{X_n Y_n} + s_3 \overline{Y_n}^2,
\end{aligned}$$

where

$$\begin{aligned}
e_1 &= z_1(hM)^2 + z_2 hM\left(u - 1 - hZ\right) + z_3(u - 1 - hZ)^2, \\
e_2 &= z_2 hMv + 2z_3\left(u - 1 - hZ\right)v, \\
e_3 &= z_3 v^2, \\
e_4 &= z_4(hM)^3 + z_5(hM)^2\left(u - 1 - hZ\right) + z_6 hM(u - 1 - hZ)^2 + z_7(u - 1 - hZ)^3, \\
e_5 &= z_5(hM)^2 v + 2z_6\left(M\right)\left(u - 1 - hZ\right)v + 3z_7(u - 1 - hZ)^2 v, \\
e_6 &= z_6\left(hM\right)v^2 + 3z_7\left(u - 1 - hZ\right)v^2, \\
e_7 &= z_7 v^3, \\
s_1 &= u_1\left(hM\right)\left(u - 1 - hZ\right) + u_2(u - 1 - hZ)^2, \\
s_2 &= u_1\left(hM\right)v + 2u_2\left(u - 1 - hZ\right)v, \\
s_3 &= u_2 v^2,
\end{aligned}$$

so

$$\begin{pmatrix} \widetilde{f}\left(\overline{X_n}, \overline{Y_n}\right) \\ \widetilde{g}\left(\overline{X_n}, \overline{Y_n}\right) \end{pmatrix} = \begin{pmatrix} \dfrac{1}{hM} & 0 \\ -\dfrac{u - 1 - hZ}{hM} & \dfrac{1}{v} \end{pmatrix} \begin{pmatrix} f\left(\overline{X_n}, \overline{Y_n}\right) \\ g\left(\overline{X_n}, \overline{Y_n}\right) \end{pmatrix}.$$

According to the central manifold theorem and the normative theory, we can get the bifurcation direction of the Hopf bifurcation at the positive equilibrium point, and according to the canonical theory of the Hopf bifurcation, make the following equation take values at $\left(\overline{X_n}, \overline{Y_n}, \delta_0\right) = (0, 0, 0)$.

$$\begin{aligned}
L &= -\mathrm{Re}\left[\frac{(1 - 2\lambda)\,\overline{\lambda}^2}{1 - \lambda} g_{11} g_{20}\right] - \frac{1}{2}|g_{11}|^2 - |g_{02}|^2 + \mathrm{Re}\left(\overline{\lambda} g_{21}\right), \\
g_{20} &= \frac{1}{8}\left(\widetilde{f}_{\overline{X_n X_n}} + \widetilde{f}_{\overline{Y_n Y_n}} + 2\widetilde{g}_{\overline{X_n Y_n}} + i\left(\widetilde{g}_{\overline{X_n X_n}} - \widetilde{g}_{\overline{Y_n Y_n}} - 2\widetilde{f}_{\overline{X_n Y_n}}\right)\right), \\
g_{11} &= \frac{1}{4}\left(\widetilde{f}_{\overline{X_n X_n}} + \widetilde{f}_{\overline{Y_n Y_n}} + i\left(\widetilde{g}_{\overline{X_n X_n}} + \widetilde{g}_{\overline{Y_n Y_n}}\right)\right), \\
g_{02} &= \frac{1}{8}\left(\widetilde{f}_{\overline{X_n X_n}} - \widetilde{f}_{\overline{X_n Y_n}} + 2\widetilde{g}_{\overline{X_n Y_n}} + i\left(\widetilde{g}_{\overline{X_n X_n}} - \widetilde{g}_{\overline{Y_n Y_n}} + 2\widetilde{f}_{\overline{X_n Y_n}}\right)\right), \\
g_{21} &= \frac{1}{16}\left(\widetilde{f}_{\overline{X_n X_n X_n}} + \widetilde{f}_{\overline{X_n Y_n Y_n}} + \widetilde{g}_{\overline{X_n Y_n Y_n}} + \widetilde{g}_{\overline{Y_n Y_n Y_n}}\right) \\
&\quad + \frac{1}{16} i\left(\widetilde{g}_{\overline{X_n X_n X_n}} - \widetilde{g}_{\overline{X_n Y_n Y_n}} - \widetilde{f}_{\overline{X_n X_n Y_n}} - \widetilde{f}_{\overline{Y_n Y_n Y_n}}\right), \\
\widetilde{f}_{\overline{X_n X_n}} &= \frac{2e_1}{hM}, \\
\widetilde{f}_{\overline{Y_n Y_n}} &= \frac{2e_3}{hM},
\end{aligned}$$

$$
\begin{aligned}
&\widetilde{f}_{\overline{X_nY_n}} = \frac{e_2}{hM},\\
&\widetilde{f}_{\overline{X_nX_nX_n}} = \frac{6e_4}{hM},\\
&\widetilde{f}_{\overline{X_nX_nY_n}} = \frac{2e_5}{hM},\\
&\widetilde{f}_{\overline{X_nY_nY_n}} = \frac{2e_6}{hM},\\
&\widetilde{f}_{\overline{Y_nY_nY_n}} = \frac{6e_7}{hM},\\
&\widetilde{g}_{\overline{X_nX_n}} = 2\left(\left(-\frac{u-1-hZ}{hM}\right)e_1 + \frac{s_1}{v}\right),\\
&\widetilde{g}_{\overline{Y_nY_n}} = 2\left(\left(-\frac{u-1-hZ}{hM}\right)e_3 + \frac{s_3}{v}\right),\\
&\widetilde{g}_{\overline{X_nY_n}} = \left(-\frac{u-1-hZ}{hM}\right)e_2 + \frac{s_2}{v},\\
&\widetilde{g}_{\overline{X_nX_nX_n}} = 6\left(-\frac{u-1-hZ}{hM}\right)e_4,\\
&\widetilde{g}_{\overline{X_nX_nY_n}} = 2\left(-\frac{u-1-hZ}{hM}\right)e_5,\\
&\widetilde{g}_{\overline{X_nY_nY_n}} = 2\left(-\frac{u-1-hZ}{hM}\right)e_6,\\
&\widetilde{g}_{\overline{Y_nY_nY_n}} = 2\left(-\frac{u-1-hZ}{hM}\right)e_7.
\end{aligned}
$$

**Theorem 4.1.** *If the above condition holds and $L \neq 0$, the Hopf bifurcation appears at the positive equilibrium point $B\,(N_0, S_0)$. If $L > 0$, it converges at that point; if $L < 0$, it diverges at that point.*

Using numerical simulations to verify the theoretical proof, we set $k = 50000$, $\eta = 1.54$, $\beta = 5.77$, $\rho = 1$, $h = 0.087593294844698$, $S_{\max} = 10$, $\delta = 0.9$, $r = 5$, $(N_0, S_0) = (4.319623064185476, 1.360753871629049)$ :

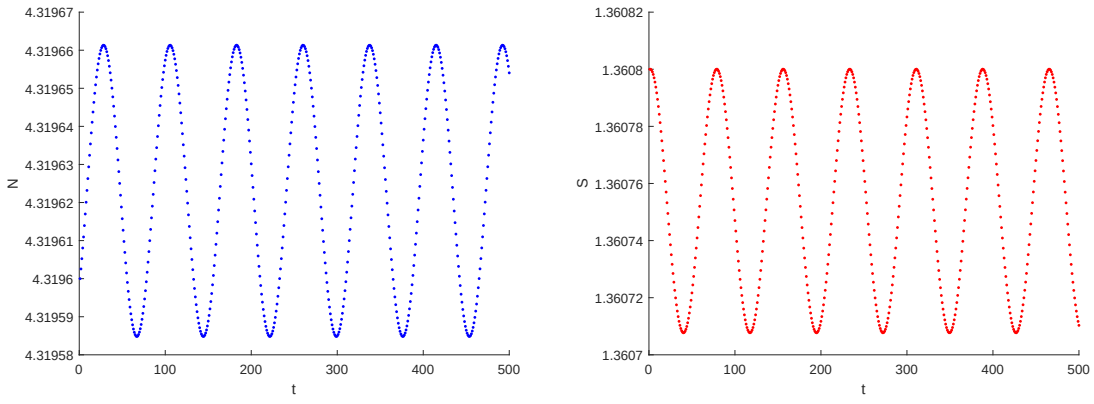


**Figure 2.** The graph of $N$, $S$ when Hopf bifurcation occurs at $k = 50000$, $\eta = 1.54$, $\beta = 5.77$, $\rho = 1$, $h = 0.087593294844698$, $S_{\max} = 10$, $\delta = 0.9$, $r = 5$, $(N_0, S_0) = (4.319623064185476, 1.360753871629049)$.

## 5. Chaotic analysis

**Definition 5.1.** For the twos systems $N_{n+1} = f(N_n)$, $S_{n+1} = f(S_n)$, if there is a small perturbation $\delta_0$ is imposed to the system, as the number of iterations increases, the system will diverge. The extent of separation is commonly used to measure the maximum Lyapunov exponent, which has the formula:

$$\lambda = \lim_{n\to+\infty} \frac{1}{n} \sum_{n=0}^{n-1} \ln \left| \frac{df(N_n, \delta_0)}{dN} \right|.$$

**Theorem 5.1.** *If $\lambda < 0$, it means that the adjacent points eventually merge into a point, which corresponds to stable fixed points and periodic motion; if $\lambda > 0$, it means that the adjacent points eventually separate, which corresponds to the local instability of the orbit, chaos occurs.*

After selecting the perturbation $\delta_0 = (0, 0.1)$, the trend of $N$ variation is analyzed using numerical simulation, and through numerical simulation, the maximum Lyapunov exponent plot is consistent with the trend of the bifurcation plot.

First we set $k = 10000$, $\eta = 7.54$, $\beta = 14.97$, $\rho = 0.9$, $h = 0.262122270347572$, $S_{\max} = 50$, $\delta = 0.6$, $r = 10$, $B(N_0, S_0) = (1.499951950752, 0.001601641574)$.

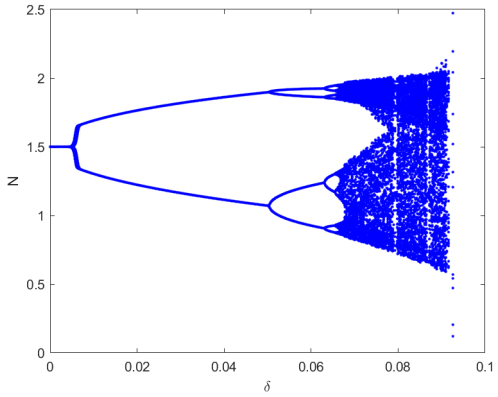


**Figure 3.** The Flip bifurcation is chaotic with the parameters $k = 10000$, $\eta = 7.54$, $\beta = 14.97$, $\rho = 0.9$, $h = 0.262122270347572$, $S_{\max} = 50$, $\delta = 0.6$, $r = 10$, $B(N_0, S_0) = (1.499951950752, 0.001601641574)$.

Then we set $k = 50000$, $\eta = 1.54$, $\beta = 5.77$, $\rho = 1$, $h = 0.087593294844698$, $S_{\max} = 10$, $\delta = 0.9$, $r = 5$. In this case, we have $(N_0, S_0) = (4.319623064185476, 1.360753871629049)$, and the Hopf bifurcation is chaotic (see Figure 5), the maximum Lyapunov exponential map is demonstrated by Figure 6.

## 6. Conclusion

The dynamic behavior of a type of spruce aphid model in discrete forest diseases and insect pests is mainly considered, we have discussed the existence of the equilibrium point in system (1.3), and found that it has three unique equilibrium points, then analyzed the stability and instability conditions. Additionally, according to the conditions where the Flip bifurcation and the Hopf bifurcation occur, we obtained the model (1.3) to experience the double cycle bifurcation (the Flip bifurcation) and the Hopf bifurcation at the positive equilibrium point $B(N_0, S_0)$. Finally,

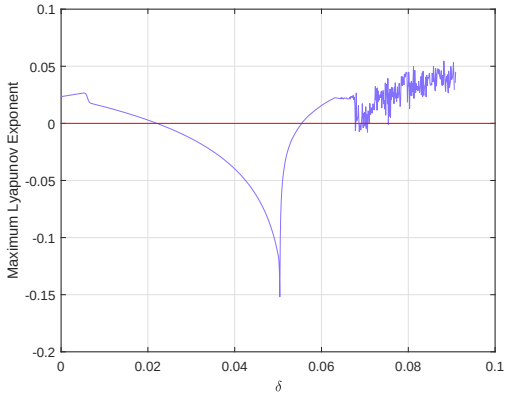


**Figure 4.** The parameters in the figure are the maximum Lyapunov exponential map where $k = 10000$, $\eta = 7.54$, $\beta = 14.97$, $\rho = 0.9$, $h = 0.262122270347572$, $S_{\max} = 50$, $\delta = 0.6$, $r = 10$, $B(N_0, S_0) = (1.499951950752, 0.001601641574)$.

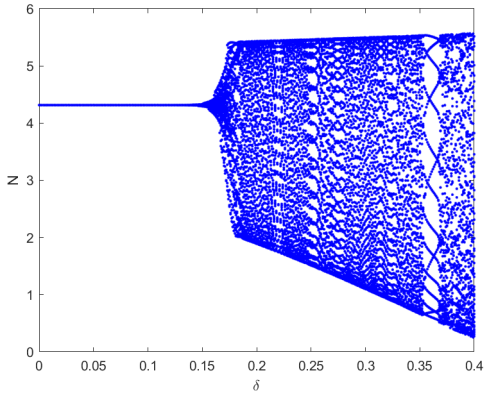


**Figure 5.** The Hopf bifurcation is chaotic with the parameters $k = 50000$, $\eta = 3.72$, $\beta = 8.47$, $\rho = 1$, $h = 0.149687409244297$, $S_{\max} = 10$, $\delta = 0.9$, $r = 5$, $B(N_0, S_0) = (4.3149528055, 1.3700943889)$.

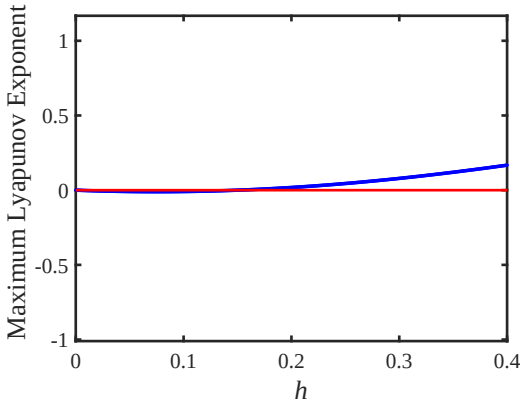


**Figure 6.** The parameters in the figure are the maximum Lyapunov exponential map where $k = 50000$, $\eta = 3.72$, $\beta = 8.47$, $\rho = 1$, $h = 0.149687409244297$, $S_{\max} = 10$, $\delta = 0.9$, $r = 5$, $B(N_0, S_0) = (4.3149528055, 1.3700943889)$.

the numerical simulation results are consistent with the theoretical predictions, and we illustrate the results of the double cycle bifurcation (Flip bifurcation) and Hopf bifurcation at the positive equilibrium point $B\left(N_0, S_0\right)$ with the corresponding figure.

## References


[1] Y. Bai, L. Wang and X. Yuan, *Pesticide control, physical control, or biological control, How to manage forest pests and diseases more effectively*, Front. Ecol. Evol., 2023, 11. DOI: 10.3389/fevo.2023.1200268.

[2] D. Bevacqua, I. Grechi, M. Génard, et al., *The consequences of aphid infestation on fruit production become evident in a multi-year perspective: Insights from a virtual experiment*, Ecol. Model., 2016, 338, 11–16.

[3] S. J. Crute, *Computer simulations of green spruce aphid populations*, J. Anim. Ecol., 1992.

[4] B. Dalziel, E. Thomann and J. Medlock, *Global analysis of a predator-prey model with variable predator search rate*, J. Math. Biol., 2020, 81(1), 159–183.

[5] K. R. Day, H. Armour and M. Docherty, *Population responses of a conifer-dwelling aphid to seasonal changes in its host*, Ecol. Entomol., 2004, 29(5), 555–565.

[6] K. R. Day, M. P. Ayres, R. Harrington, et al., *Interannual dynamics of aerial and arboreal green spruce aphid populations*, Popul. Ecol., 2010, 52, 317–327.

[7] S. A. Estay, M. Lima, F. A. Labra, et al., *Increased outbreak frequency associated with changes in the dynamic behaviour of populations of two aphid species*, Oikos, 2012, 121(4), 614–622.

[8] B. Hong and C. Zhang, *Bifurcations and chaotic behavior of a predator-prey model with discrete time*, AIMS Math., 2023, 8(6), 13390–13410.

[9] Y. L. Huang, W. Y. Shi and S. W. Zhang, *A stochastic predator-prey model with Holling II increasing function in the predator*, J. Biol. Dyn., 2021, 15(1), 1–18.

[10] S. R. J. Jang and D. M. Johnson, *Dynamics of discrete-time larch budmoth population models*, J. Biol. Dyn., 2009, 3(2–3), 209–223.

[11] L. Ji, Z. Wang, X. Wang, et al., *Forest insect pest management and forest management in China: An overview*, Environ. Manage., 2011, 48, 1107–1121.

[12] J. T. Jones, M. Moens, M. Mota, et al., *Bursaphelenchus xylophilus: Opportunities in comparative genomics and molecular host–parasite interactions*, Mol. Plant Pathol., 2008, 9(3), 357–368.

[13] G. Lemperiere, K. R. Day, Y. Petit-Berghem, et al., *Interannual population dynamics of the green spruce aphid Elatobium abietinum (Walker) in France*, Ann. Appl. Biol., 2020, 176(3), 233–240.

[14] A. H. Li, H. Y. Jing and J. C. Fu, *Dynamic characteristic of spruce budworm–its natural enemy–pesticide interaction model*, J. Biomathem., 2006, 21(3), 377–383.

[15] T. Li, X. Zhang and C. Zhang, *Pattern dynamics analysis of a space–time discrete spruce budworm model*, Chaos. Solitons. Fractals., 2024, 179, 114423.

[16] L. Liang, S. Niu and J. Wang, *Current situation and future study on effect of invading Bursaphelenchus xylophilus on ecosystem*, J. Zhejiang For. Sci. Technol., 2006, 73–78.

[17] M. Lima, R. Harrington, S. Saldaña, et al., *Non-linear feedback processes and a latitudinal gradient in the climatic effects determine green spruce aphid outbreaks in the UK*, Oikos, 2008, 117(6), 951–959.

[18] D. Ludwig, D. D. Jones and C. S. Holling, *Qualitative analysis of insect outbreak systems: The spruce budworm and forest*, J. Anim. Ecol., 1978, 47(1), 315–332.

[19] C. W. Luo and K. Li, *The relation of species diversity to pest control in forest plantations*, Sci. Silv. Sin., 2006, 109–115.

[20] A. Rasmussen, J. Wyller and J. O. Vik, *Relaxation oscillations in spruce–budworm interactions, nonlinear analysis: Real world applications*, Chin. J. Biol. Control, 2011, 304–319.

[21] S. Redlich, J. Clemens, M. K. F. Bader, et al., *Identifying new associations between invasive aphids and Pinaceae trees using plant sentinels in botanic gardens*, Biol. Invas., 2019, 21, 217–228.

[22] J. H. M. Thornley and J. A. Newman, *Climate sensitivity of the complex dynamics of the green spruce aphid—Spruce plantation interactions: Insight from a new mechanistic model*, Plos. One, 2022, 17(2), e0252911.

[23] D. W. Williams and A. M. Liebhold, *Spatial scale and the detection of density dependence in spruce budworm outbreaks in eastern North America*, Oecologia, 2000, 124, 544–552.

[24] D. W. Williams and A. M. Liebhold, *Spatial synchrony of spruce budworm outbreaks in eastern North America*, Ecology, 2000, 81(10), 2753–2766.

[25] H. C. Xu and Y. Q. Luo, *Ecosystems attacked by Bursaphelenchus xylophilus: A review*, J. Zhejiang For. Coll., 2010, 27(3), 445–450.

[26] J. Xu and S. Yuan, *Near-optimal control of a stochastic pine wilt disease model with prevention strategies*, Math. Methods Appl. Sci., 2023, 46(13), 13855–13881.

[27] Q. Xu and C. Zhang, *Bifurcation analysis and chaos of a modified Holling-Tanner model with discrete time*, J. Appl. Anal. Comput., 2024, 14(6), 3425–3449.

[28] W. Xu, S. Chen and L. Chen, *Modeling of the prevention and control of forest pest*, J. Biol. Syst., 2007, 15(04), 539–550.

[29] M. Yang, M. Li, L. Qu, et al., *Advances in research on pathogenic microorganisms of pine sawfly*, Chin. J. Biol. Control, 2007, 23(3), 284–289.

[30] Z. Yang, X. Wang, Y. Zhang, et al., *Research advances of Chinese major forest pests by integrated management based on biological control*, Chin. J. Biol. Control., 2018, 34(2), 163.

[31] X. Zhang, C. Zhang and Y. Zhang, *Pattern dynamics analysis of a time-space discrete FitzHugh-Nagumo (FHN) model based on coupled map lattices*, Comput. Math. Appl., 2024, 157, 92–123.

[32] X. Zhang, C. Zhang and Y. Zhang, *Discrete kinetic analysis of a general reaction-diffusion model constructed by Euler discretization and coupled map lattices*, Math. Comput. Simul., 2024, 1218–1236.

[33] J. Zhao and Y. Yan, *Stability and bifurcation analysis of a discrete predator–prey system with modified Holling–Tanner functional response*, Adv. Differ. Equ., 2018, 2018(1), 402.

[34] J. Zheng, Y. Xu, H. Zhang, et al., *Advances and prospects of target recognition techniques for forest pest control at home and abroad*, Sci. Silv. Sin., 2023, 152–166.

Received December 2024; Accepted July 2025; Available online August 2025.